Sessile droplets with negative line tension

Luca Guzzardi

Dipartimento di Matematica, Università di Firenze,

Viale Morgagni 67a, 50134 Firenze, Italy,

and Istituto Nazionale di Fisica della Materia,

Università di Pavia, Via Ferrata 1, 27100 Pavia, Italy

Riccardo Rosso and Epifanio G. Virga

Dipartimento di Matematica, Istituto Nazionale di Fisica della Materia,

Università di Pavia, Via Ferrata 1, 27100 Pavia, Italy

(Dated: January 19, 2005)

Abstract

Abstract: We study the local stability of a sessile droplet with non-vanishing line tension along the contact line, where three phases are in equilibrium. We confirm Widom's results [5] on the local stability of a droplet with positive line tension in a larger class of perturbations. When the line tension is negative, although equilibria would be unstable against modes that make the contact line wigglier and wigglier, the length over which the oscillations of destabilizing modes are effective can become too short compared ti the natural cut-off length given by the ratio between the line and the surface tensions of the droplet. Thus, provided that the line tension strength is not too large, conditionally stable equilibria exist, even when the line tension is negative.

PACS numbers: 68.08.Bc

I. INTRODUCTION

Stability of sessile droplets is a major topic in wetting science. Although this is a topic with a long history, in the past few years it has received renewed attention because new challenges have been posed by the availability of experimental techniques to explore reliably small length-scales in the micrometer range, and by the urge of technological applications in nanofluids. Section 2 of [1] reviews applications that directly involve line tension effects. As a consequence, the classical problem of finding the equilibrium of a sessile droplet on a flat, homogeneous substrate has been revived, and a plethora of new challenging phenomena, interesting both physicists and mathematicians, has been revealed. Here we are mostly concerned with the effects of line tension on the equilibrium and stability of droplets. Line tension was originally introduced by Gibbs in his seminal paper [2], by analogy with surface tension. In fact, as the surface tension measures the excess free energy along an interface separating two distinct phases, the line tension measures the excess free energy along a contact line where three distinct phases coexist in equilibrium. In [2], Gibbs also heeded an important difference between surface and line tensions: while the former must be positive, the latter can have either sign. Accounting for the line tension has effects on the equilibrium of droplets, since Young equation, which governs the shape of the contact line, is altered. The generalized Young equation establishes a relation between the line tension and the droplet's contact angle, which also involves the geometric properties of the contact line. Line tension measurements are based upon this equation, but for several reasons—above all, the small length-scales at which the effects of line tension are perceptible—they provided values differing from one another by several orders of magnitude. Even worse, no consensus has been achieved upon the sign of the line tension. The main theoretical objection against negative values of the line tension is that the free-energy functional—whose minima should represent stable, and hence observable, equilibria—is unbounded from below, so that every equilibrium configuration can be made unstable, by suitably selecting a perturbing mode (see, *e.g.* [3] and [4]). The crucial point, however, is to determine the typical length-scale associated with destabilizing modes. If this length is below the range of validity of the model, the instability has a purely mathematical meaning with no physical counterpart, since it is effective where the model needs corrections that, plausibly, will automatically remove the pathological behaviour of the functional. On the other hand, even the hypothesis of constant surface tension is tenable only if the size of the droplet is much larger than the range of intermolecular forces [5] and indeed curvature corrections have been considered for surface tension (see *e.g.* [6] for a recent contribution along these lines). Similar corrections were introduced long ago for line

tension too [7], but this formal theory has too many parameters to be handled comfortably. Here we follow a different avenue which relies upon a stability criterion worked out in [8] and applied in [9] to explore the stability of liquid bridges in the presence of line tension. This criterion is general enough to cover line tension effects as well as inhomogeneities and arbitrary geometries of the substrate. These features make it more flexible than Lenz and Lipowsky's criterion [10], which did not include line tension effects and was not applicable to curved substrates. Also Sekimoto, Oguma and Kawasaki [16] had performed a stability analysis, to which we will refer later in this paper. While they covered several wetting morphologies, by considering even doughnut droplets, their analysis was restricted to homogeneous, flat substrates and, more importantly, it was confined to small contact angles, while no similar restriction is imposed in [8].

We consider a sessile droplet lying on a homogeneous, rigid, flat substrate, in the presence of line tension. This problem was examined by Widom in [5], to which we will often refer in the sequel. Widom compared the free energy of a sessile droplet having a nonzero line tension with that of a free sphere having the same volume, and with that of a completely wetted substrate. He found a first-order drying transition occurring when the line tension exceeds a positive critical value. For negative line tensions the sessile droplet is locally stable with respect to perturbations that preserve the spherical shape of its surface. For positive line tensions, Widom also computes the limits of metastability for a sessile droplet, in the same restricted class. Our stability criterion, which is based on a local analysis is only suitable to detect metastability limits, and so we cannot follow first-order phase transitions. However, the criterion we adopt is flexible enough to examine local stability of a sessile droplet against more general perturbations than that examined by Widom. As a result, while we can confirm Widom's conclusions on metastability limits when the line tension is positive, we prove that Widom's class of perturbations is too meagre to detect the unstable modes when the line tension is negative. In this case, we complete the stability analysis by imposing a constraint on the admissible perturbations: these are the ones effective on a length-scale larger than the typical length hidden in the problem, that is, the ratio between the line and the surface tensions. In this way we are able to prove that negative values of the line tension are compatible with stable equilibria, provided that the strength of the line tension is not too high. Our conclusions confirm those obtained in the simpler geometry of liquid bridges, but the criterion adopted here to select the effective perturbations is subtler than that employed in [9].

This paper is organized as follows. Section 2 is devoted to study the generalized Young equation: when the line tension is positive, either two or no equilibria can exist; when the line tension is negative, only one equilibrium exists. Section 3 concerns the stability of these equilibria. After a

technical premise, where the stability criterion we employ is recalled and applied to the problem at hand, we organize our results in two distinct subsections. In the one, we consider the stability of droplets with negative line tension. This subsection contains the main results of the paper: we prove that, when the strength of the line tension is not too large, an equilibrium configuration remains *conditionally* stable, as the destabilizing modes are effective only at length-scales that fall outside the range of validity of the model adopted. The other subsection concerns the stability of droplets with positive line tension: the results obtained by Widom [5] are essentially confirmed by our analysis.

In Section 4, we interpret the outcomes of Section 3 in the relevant physical parameters. Finally, a closing section summarizes the contents of the paper and indicates the prospects of future work.

II. EQUILIBRIA

Here we find the equilibrium configurations of a droplet $\mathcal{B}$ lying on a rigid, fixed substrate. We assume that the droplet consists of an incompressible fluid, so that it has a constant volume V. The boundary $\partial\mathcal{B}$ of $\mathcal{B}$ can be split as $\partial\mathcal{B} = \mathcal{S} \cup \mathcal{S}_*$, where the free surface $\mathcal{S}$ is in contact with the environment fluid, while the adhering surface $\mathcal{S}_*$ is in contact with the substrate. The surfaces $\mathcal{S}$ and $\mathcal{S}_*$ meet along the contact line $\mathcal{C}$ where, in fact, three different phases coexist. The equilibrium configurations of the droplet $\mathcal{B}$ solve the Euler equation associated with the free-energy functional $\mathcal{F}$ defined by

$$\mathcal{F}[\mathcal{B}] = \gamma \int_{\mathcal{S}} \mathrm{d}a + (\gamma - w) \int_{\mathcal{S}_*} \mathrm{d}a + \tau \int_{\mathcal{C}} \mathrm{d}s, \tag{1}$$

where the positive constant γ is the *surface tension* associated with the interface $\mathcal{S}$ between the droplet and the surrounding fluid, $w > 0$ is the *adhesion potential* that characterizes the affinity between the droplet and the substrate, and τ is the *line tension* introduced to account for the excess free energy concentrated along the contact line $\mathcal{C}$. We also note that, in (1), a denotes the area measure on both $\mathcal{S}$ and $\mathcal{S}_*$, and s is the arc-length along $\mathcal{C}$. At variance with γ and w, which are positive, the line tension τ can be either positive or negative: the very objective of this paper is to study how the sign of τ affects the stability of the equilibria of $\mathcal{B}$.

By taking (1) as the free energy of the droplet $\mathcal{B}$, we are tacitly making several assumptions. Indeed, we neglect body forces like gravity and, by taking w a constant, we also assume that the substrate is chemically homogeneous. Finally, we suppose that the line tension does not depend on the geometry of the contact line. While dropping any of these hypotheses has no effect on

the validity of the methods we employ, assuming them contribute to keep computations at an acceptable level of difficulty.

The Euler equation associated with (1) has been derived numberless times (see *e.g.* [8]): it requires that the free surface $\mathcal{S}$ has constant mean curvature. Since the contact line is not fixed, the following natural boundary condition, which generalizes the classical Young equation, holds along $\mathcal{C}$:

$$\gamma \cos\vartheta_c + \gamma - w - \tau\kappa_g^* = 0\,, \quad \text{along } \mathcal{C}. \tag{2}$$

Here ϑ_c is the *contact angle*, that is, the angle between the droplet's and the substrate's conormal unit vectors at the contact line $\mathcal{C}$ (see Fig. 1), and κ_g^* is the geodesic curvature of $\mathcal{C}$, thought of as a curve on the substrate $\mathcal{S}^*$. We heed that in [5] the contact angle was chosen as $\pi - \vartheta_c$.

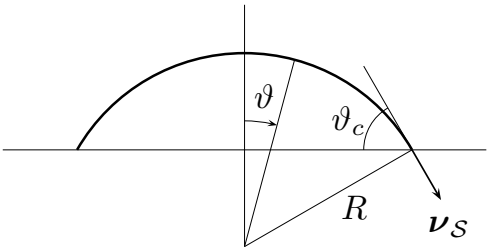

FIG. 1: Cross-section of a spherical droplet with radius R lying on a flat, homogeneous substrate. The angle ϑ denotes the colatitude on the droplet's surface, and ϑ_c is the contact angle, that is, the angle between the droplet's and the substrate's conormals.

Among surfaces with constant mean curvature, we focus our attention on free surfaces $\mathcal{S}$ that are spherical caps of radius R. As a further simplification, we assume that the substrate is *flat*, whence it follows that the contact line $\mathcal{C}$ is a circle with radius $R\sin\vartheta_c$, and so its geodesic curvature on $\mathcal{S}^*$ is (see *e.g.* p. 249 of [11])

$$\kappa_g^* = -\frac{1}{R\sin\vartheta_c}\,.$$

Finally, the volume V of the droplet $\mathcal{B}$ depends only on R and ϑ_c according to the formula

$$V = \frac{\pi R^3}{3}[2 + (\cos\vartheta_c)^3 - 3\cos\vartheta_c]\,. \tag{3}$$

The dependence of κ_g^* on R and ϑ_c, which are further related through equation (3), makes it non trivial resolving (2). For future use, it is expedient to recast (2) in a dimensionless form. To this aim we note that, if $(w-\gamma)/\gamma \in [-1,1]$, then it is possible to define the *bare* contact angle ϑ_c^0 as

$$\cos\vartheta_c^0 := \frac{w-\gamma}{\gamma}\,. \tag{4}$$

Hence, ϑ_c^0 represents the contact angle at the equilibrium, in the absence of line tension. The line tension τ introduces a typical length-scale $|\xi|$ into the model, with

$$\xi := \frac{\tau}{\gamma}\,. \tag{5}$$

As we shall see, the ratio between ξ and the typical size of the droplet plays a major rôle in determining whether an equilibrium is stable or not. Thus, we also introduce the dimensionless ratios

$$\varepsilon := \frac{\xi}{R} \tag{6}$$

and

$$\delta := \frac{3V}{\pi\xi^3}\,, \tag{7}$$

which will be used repeatedly in the sequel. We finally stress that ξ, ε, and δ inherit their sign from the line tension τ. By using equations (4)-(7) we rephrase (2) and (3) as

$$\begin{cases} \varepsilon = \sin\vartheta_c(\cos\vartheta_c^0 - \cos\vartheta_c) =: \varepsilon_1(\vartheta_c, \vartheta_c^0) \\ \varepsilon = \sqrt[3]{\frac{2+(\cos\vartheta_c)^3 - 3\cos\vartheta_c}{\delta}} =: \varepsilon_2(\vartheta_c, \delta)\,, \end{cases} \tag{8}$$

provided that $\vartheta_c \in (0,\pi)$ and $\delta \neq 0$. Excluding $\vartheta_c = 0$ and $\vartheta_c = \pi$ simply means that we are in a partial wetting regime, away from both the wetting transition ($\vartheta_c = 0$) and the drying transition ($\vartheta_c = \pi$). On the other hand, the value $\delta = 0$ can be recovered in the limit as the line tension diverges.

The function $\varepsilon_1(\vartheta_c, \vartheta_c^0)$ depends continuously on the bare contact angle ϑ_c^0, whereas $\varepsilon_2(\vartheta_c, \delta)$ depends continuously on $\delta \neq 0$. When ϑ_c^0 ranges in $[0,\pi]$, the curves $\varepsilon_1(\vartheta_c, \vartheta_c^0)$ span the shaded region $\mathcal{A}$ in Fig. 2, with the upper curve corresponding to $\vartheta_c^0 = 0$, and the lower curve to $\vartheta_c^0 = \pi$. We also note that the slope of $\varepsilon_1(\vartheta_c, \vartheta_c^0)$ at $\vartheta_c = 0$ is non-positive, being zero only if $\vartheta_c^0 = 0$. Graphs of the functions in the family $\varepsilon_2(\vartheta_c, \delta)$ always pass through the origin of the $(\vartheta_c, \varepsilon)$-plane and, for all admissible values of δ, satisfy $\lim_{\vartheta_c \to 0} \varepsilon_2'(\vartheta_c, \delta) = 0$, where a prime stands for differentiation with respect to ϑ_c. If $\delta > 0$, the functions $\varepsilon_2(\vartheta_c, \delta)$ are monotonically increasing, while they are monotonically decreasing, if $\delta < 0$. Whenever the graph of a function $\varepsilon_2(\vartheta_c, \delta)$ lies inside $\mathcal{A}$, there is at least one value of ϑ_c^0 that solves (8). Conversely, for every point P in $\mathcal{A}$, there is at least a pair $(\overline{\vartheta}_c^0, \overline{\delta})$ such that $\varepsilon_1(\vartheta_c, \overline{\vartheta}_c^0)$ and $\varepsilon_2(\vartheta_c, \overline{\delta})$ intersect each other at P, and so solve (8).

The pair $\vartheta_c = 0$, $\varepsilon = 0$ always solves (8), but it is a spurious solution that appears when (2) is multiplied by $\sin\vartheta_c$ to arrive at $(8)_1$. When $\delta > 0$, and the bare contact angle has a prescribed

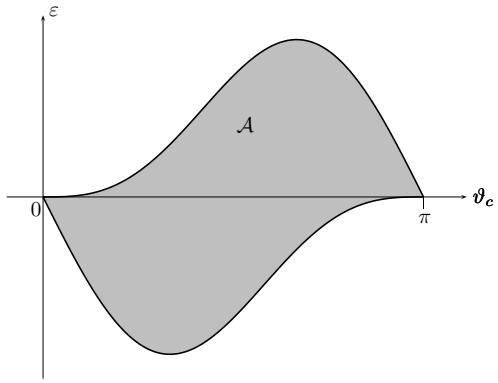

FIG. 2: The admissible region $\mathcal{A}$ is the region of the $(\vartheta_c, \varepsilon)$-plane where equations (8) can be solved.

value ϑ_c^0, two more solutions exist provided that δ ranges in the interval $(\delta_c(\vartheta_c^0), +\infty)$, where $\delta_c(\vartheta_c^0)$ is determined by (8) and the condition that $\varepsilon_1'(\vartheta_c, \vartheta_c^0) = \varepsilon_2'(\vartheta_c, \delta_c(\vartheta_c^0))$ at the point where (8) holds. If $\delta \in (0, \delta_c(\vartheta_c^0))$, (8) has no acceptable solution, and so no equilibrium exists. This shows that even in a simple geometry, adding a contribution from line tension makes the modified Young equation nontrivial. When $\delta < 0$, a unique solution different from $\vartheta_c = 0$, $\varepsilon = 0$ exists for any prescribed value of ϑ_c^0, as can be easily proved by recalling that, while $\varepsilon_1(0, \vartheta_c^0) = \varepsilon_1(\pi, \vartheta_c^0) = 0$, and $\varepsilon_1'(0, \vartheta_c^0) < 0$, the function $\varepsilon_2(\vartheta_c, \delta)$ is such that $\lim_{\vartheta_c \to 0} \varepsilon_2(\vartheta_c, \delta) = 0$, it is monotonically decreasing in ϑ_c and, moreover, $\lim_{\vartheta_c \to 0} \varepsilon_2'(\vartheta_c, \delta) = 0$. Figure 3 shows the possible scenarios outlined here,

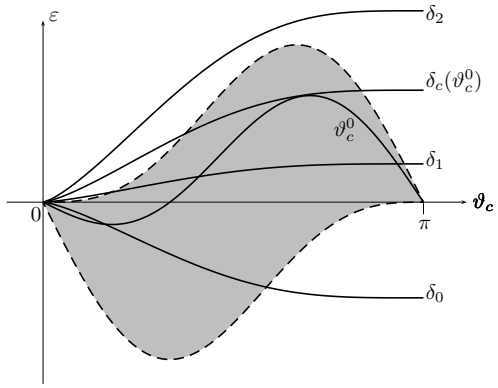

FIG. 3: Graphical solution of the system (8), for a given value of ϑ_c^0. Together with the admissible region $\mathcal{A}$ (in gray) we plotted the curve $\varepsilon_1(\vartheta_c, \vartheta_c^0)$, and several curves in the family $\varepsilon_2(\vartheta_c, \delta)$. When $\delta \in (\delta_c(\vartheta_c^0), +\infty)$ (*e.g.* the curve with $\delta = \delta_1$), two acceptable equilibria exist, while no equilibrium exists for $\delta \in (0, \delta_c(\vartheta_c^0))$ (*e.g.* the curve with $\delta = \delta_2$). At $\delta = \delta_c(\vartheta_c^0)$ the two equilibria coalesce into a unique equilibrium solution. On the other hand, when δ is negative (*e.g.* the curve with $\delta = \delta_0$), a unique equilibrium exists.

for a prescribed value of ϑ_c^0. As a final remark, we obtain from $(8)_1$ that the equilibrium contact angle ϑ_c is larger than the bare contact angle ϑ_c^0, when the line tension is positive, whereas it is

smaller than ϑ_c^0, when the line tension is negative. We also heed that, by $(8)_2$, in the limit where the line tension is negative and divergent, and so $\delta \to -\infty$, the equilibrium contact angle migrates towards 0. In the next section we will study the effects of negative line tension on the stability of the equilibrium solutions obtained here.

III. STABILITY

To obtain the Euler equation and the generalized Young equation (2) dictating the equilibrium shape of the droplet $\mathcal{B}$ we only needed to compute the first variation $\delta\mathcal{F}$ of the functional $\mathcal{F}$, by perturbing the points p on $\mathcal{B}$ as follows

$$p \mapsto p_\varepsilon := p + \varepsilon \boldsymbol{u}\,, \tag{9}$$

then setting

$$\delta\mathcal{F}[\boldsymbol{u}] := \left.\frac{\mathrm{d}\mathcal{F}[\boldsymbol{u}]}{\mathrm{d}\varepsilon}\right|_{\varepsilon=0} = 0\,.$$

To assess the local stability of an equilibrium configuration, however, the sign of the second variation

$$\delta^2\mathcal{F} := \left.\frac{\mathrm{d}^2\mathcal{F}[\boldsymbol{u}]}{\mathrm{d}\varepsilon^2}\right|_{\varepsilon=0}$$

needs be evaluated. In [8] we proved that, in general, the perturbation (9) is not suitable to keep the constraints involved in the problem up to second order in ε. In particular, we pointed out that, to account properly for the gliding of a droplet on an arbitrarily curved substrate, a point p on $\mathcal{B}$ must be mapped into

$$p_\varepsilon := p + \varepsilon\boldsymbol{u} + \varepsilon^2\boldsymbol{v}\,, \tag{10}$$

with the fields $\boldsymbol{u}$ and $\boldsymbol{v}$ constrained to obey

$$\boldsymbol{u}\cdot\boldsymbol{\nu}_* = 0 \qquad \text{and} \qquad \boldsymbol{v}\cdot\boldsymbol{\nu}_* = -\frac{1}{2}\boldsymbol{u}\cdot(\nabla_{\mathrm{s}}\boldsymbol{\nu}_*)\boldsymbol{u} \qquad \text{on } \mathcal{S}_*\,, \tag{11}$$

where $\boldsymbol{\nu}_*$ is the unit normal vector to the substrate, properly oriented (*see* p. 3992 of [8]) and $\nabla_{\mathrm{s}}\boldsymbol{\nu}_*$ is its surface-gradient (*see* Appendix B of [8]). While the field $\boldsymbol{v}$ does not modify the equilibrium equations, it plays a rôle in the second variation: in particular, the use of $(11)_2$ together with the equilibrium equations makes it possible to write the second variation as a quadratic functional depending only upon the component $u := \boldsymbol{u}\cdot\boldsymbol{\nu}$ of the field $\boldsymbol{u}$ along the outer unit normal vector $\boldsymbol{\nu}$ to the free surface $\mathcal{S}$. As usual, once the second variation $\delta^2\mathcal{F}$ is known, we minimize it on the set

$$\int_{\mathcal{S}} u^2 \mathrm{d}a = 1 \tag{12}$$

and require its minimum to be positive, to guarantee local stability of an equilibrium configuration. Besides the constraint (12), the perturbation u must preserve the volume of the droplet and so it must also obey the requirement

$$\int_{\mathcal{S}} u \mathrm{d}a = 0\,. \tag{13}$$

The integral constraints (12) and (13) are accounted for by introducing suitable multipliers $-\mu/2$ and λ, and then finding the minimum of (*cf.* pp. 4001-4002 of [8])

$$F[u] := \frac{1}{2}\int_{\mathcal{S}} \{|\nabla_{\mathrm{s}} u|^2 + \alpha u^2\}\mathrm{d}a + \lambda \int_{\mathcal{S}} u \mathrm{d}a - \frac{1}{2}\mu \int_{\mathcal{S}} u^2 \mathrm{d}a + \frac{1}{2}\int_{\mathcal{C}} \{\xi u_{s*}'^2 - \beta u_{s*}^2\}\mathrm{d}s\,, \tag{14}$$

where a prime stands for differentiation with respect to the arc-length s on $\mathcal{C}$. In (14),

$$\alpha := 2K - H^2 \tag{15}$$

depends on the total and the Gaussian curvatures H and K of $\mathcal{S}$, while u_{s*} is related to u through

$$u_{s*} = \frac{u}{\sin\vartheta_c}\,.$$

Finally,

$$\gamma\beta := \tau(K^* + \kappa_g^{*2}) + \gamma[H^* \sin\vartheta_c + H\cos\vartheta_c \sin\vartheta_c + \kappa_g(\sin\vartheta_c)^2]\,, \tag{16}$$

where H^* and K^* are the total and the Gaussian curvatures of $\mathcal{S}_*$, κ_g and κ_g^* are the geodesic curvatures of the contact line $\mathcal{C}$, conceived as a curve on $\mathcal{S}$ and $\mathcal{S}_*$, respectively. Definitions (15) and (16) are indeed special cases of the general definitions given in Sections 3 and 4 of [8], where the effects of inhomogeneities in the chemical composition of the substrate, nonconstant line tension, and geometric microstructures were also taken into account. Since for a spherical cap of radius R lying on a flat substrate $H = 2/R$, $K = 1/R^2$, $H^* = 0$, and $K^* = 0$, while for the circular contact line $\mathcal{C}$ $\kappa_g = -\cot\vartheta_c/R$ and $\kappa_g^* = -1/R\sin\vartheta_c$, by using the same analysis as in Section 4 of [8], the equilibrium equations for $F[u]$ are easily arrived at:

$$\Delta_s u + (\mu + 2)u = \lambda \quad \text{on } \mathcal{S} \tag{17}$$

and

$$\left[\frac{\partial u}{\partial\vartheta} - \frac{\varepsilon}{(\sin\vartheta_c)^4}\frac{\partial^2 u}{\partial\varphi^2} - \frac{1}{(\sin\vartheta_c)^2}\left(\frac{\varepsilon}{(\sin\vartheta_c)^2} + \sin\vartheta_c\cos\vartheta_c\right)u\right]\Big|_{\vartheta=\vartheta_c} = 0 \quad \text{along } \mathcal{C}, \tag{18}$$

where the differential operator

$$\Delta_s := \frac{1}{R^2}\frac{\partial^2}{\partial\vartheta^2} + \frac{1}{R^2}\cot\vartheta\frac{\partial}{\partial\vartheta} + \frac{1}{(R\sin\vartheta)^2}\frac{\partial^2}{\partial\varphi^2}$$

is the surface-Laplacian on the sphere, expressed in terms of the colatitude $\vartheta \in [0, \vartheta_c]$ (*see* Fig. 1) and the azimuth $\varphi \in [0, 2\pi)$. The minimum eigenvalue $\mu_{\min}$ of equations (17) and (18) coincides with the minimum value of $\delta^2\mathcal{F}$ on the set (12), whence we conclude that a configuration is unstable if $\mu_{\min}$ is negative, and locally stable if $\mu_{\min}$ is positive.

The spectrum of the surface-Laplacian on a spherical cap has been studied intensively, because it enters the solution of many applied problems in fluid dynamics and elasticity. In particular, Baginski [12] obtained upper and lower bounds on the eigenvalues of the surface-Laplacian, subject to Dirichlet boundary conditions along the contour $\mathcal{C}$. The problem we need study differs from Baginski's since we impose mixed—or Robin— boundary conditions along $\mathcal{C}$. Moreover, the presence of the multiplier λ makes the bulk equation (17) inhomogeneous.

To find $\mu_{\min}$ or, at least, to determine its sign, it is expedient to expand the solution $\overline{u}$ of the homogenous problem

$$\Delta_s \overline{u} + (\mu + 2)\overline{u} = 0 \qquad \text{on } \mathcal{S} \tag{19}$$

as

$$\overline{u} = \sum_{m=0}^{\infty} a_m u_m(\vartheta) \mathrm{trig}(m\varphi)\,, \tag{20}$$

where

$$\mathrm{trig}(m\,\varphi) := \begin{cases} \sin(m\varphi) \quad \text{or} \quad \cos(m\varphi) & \text{if } m \neq 0 \\ 1 & \text{if } m = 0, \end{cases}$$

and $a_m \in \mathbb{R}$ are the coefficients of the expansion. Using a standard procedure, we insert the expansion (20) into (19) to conclude that, for every value of m, the function $u_m(\vartheta)$ solves the equation

$$\frac{1}{\sin\vartheta}\frac{\mathrm{d}}{\mathrm{d}\vartheta}\left[\sin\vartheta\frac{\mathrm{d}u_m}{\mathrm{d}\vartheta}\right] + \left[\mu + 2 - \left(\frac{m}{\sin\vartheta}\right)^2\right] u_m = 0\,. \tag{21}$$

By selecting the solution of (21) that is bounded everywhere on $\mathcal{S}$, we are left with the associated Legendre function of the first kind $P_\nu^m(\cos\vartheta)$, where the index ν is related to μ by

$$\nu(\nu+1) = \mu + 2\,. \tag{22}$$

Equation (21) can be solved also for complex values of ν. Since the product $\nu(\nu+1)$ is invariant under the transformation $\nu \mapsto -(1+\nu)$, we can restrict attention to the values of ν with real part $\Re e(\nu) \geq -\frac{1}{2}$. Moreover, since the product $\nu(\nu+1)$ is left unchanged when the imaginary part $\Im m(\nu)$ of ν is mapped into $-\Im m(\nu)$, we can also assume $\Im m(\nu) \geq 0$.

Besides these general remarks, we need to solve equation (21) only when μ is a real number, which amounts to require either

$$\Im m(\nu) = 0 \qquad \text{or} \qquad \Re e(\nu) = -\frac{1}{2}\,.$$

Collecting all this information we conclude that the parameter ν ranges in the set $\mathcal{I}$ of the complex ν-plane shown in Figure 4, and formally defined as

$$\mathcal{I} := \left\{ \nu \in \left[-\frac{1}{2} + \mathrm{i}0\,,\, -\frac{1}{2} + \mathrm{i}\infty \right) \cup \left[-\frac{1}{2}\,,\, +\infty \right) \right\}\,.$$

As mentioned before, instability occurs when $\mu < 0$, that is, when $\Re e(\nu) < 1$ or when

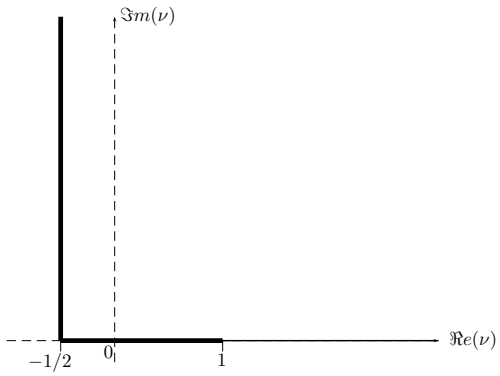

FIG. 4: Complex values of ν relevant to our analysis. The real and the imaginary axes of the complex ν-plane are dashed lines; the set $\mathcal{I}$ is a solid line, whose thicker part represents the subset $\mathcal{U}$ that corresponds to negative values of the multiplier μ and, hence, to unstable equilibria.

$$\nu \in \mathcal{U} := \left\{ \left[-\frac{1}{2} + \mathrm{i}0\,,\, -\frac{1}{2} + \mathrm{i}\infty \right) \cup \left[-\frac{1}{2}\,,\, 1 \right) \right\}\,. \tag{23}$$

As an aside, we recall that the associated Legendre functions $P_\nu^m(\cos\vartheta)$ are also called *spherical* functions when ν is real, and *conical* functions when $\nu = -\frac{1}{2} + \mathrm{i}\lambda$, with $\lambda > 0$.

The solution u of (17) differs from $\overline{u}$ by a constant c related to the multipliers λ and μ through

$$(\mu + 2)c = \nu(\nu + 1)c = \lambda\,, \tag{24}$$

provided that $\mu \neq -2$ or, equivalently, $\nu \neq 0$. We note, however, that u must satisfy the incompressibility constraint (13) that now reads as

$$\int_0^{\vartheta_c} \int_0^{2\pi} u(\vartheta, \varphi) \sin\vartheta \mathrm{d}\vartheta \mathrm{d}\varphi = 0\,. \tag{25}$$

Since we are performing a modal analysis, and so we look for the conditions that make a specific mode unstable, we adjust the constraint mode by mode, by adding to the function

$$u_m(\vartheta, \varphi) := P_\nu^m(\cos\vartheta)\mathrm{trig}(m\,\varphi) \qquad m \in \mathbb{N}$$

a constant $c(\vartheta_c, \nu, m)$ that makes the constraint obeyed, so that λ follows from (24), apart from the case $\nu = 0$ that needs a separate treatment.

The factor trig$(m\varphi)$ guarantees that $u_m(\vartheta, \varphi)$ automatically obeys the constraint (25) when $m > 0$, and so both $c(\vartheta_c, \nu, m)$ and the corresponding value of λ vanish. When $m = 0$, we proceed as follows. First, we recall the relation (see equation (7.8.3) of [13])

$$P'_{\nu+1}(x) - xP'_\nu(x) = (\nu + 1)P_\nu(x)\,, \tag{26}$$

where we have omitted the superscript 0 in the Legendre functions, and a prime stands for differentiation with respect to the argument. Second, noting that

$$\int_0^{\vartheta_c}\int_0^{2\pi} P^0_\nu(\cos\vartheta)\sin\vartheta \mathrm{d}\vartheta d\varphi = 2\pi\int_{x^c}^1 P^0_\nu(x)\mathrm{d}x\,,$$

where $x_c := \cos\vartheta_c$, by integrating (26) by parts and recalling that $P_\nu(1) = 1$ for all values of ν, we obtain

$$\int_0^{\vartheta_c}\int_0^{2\pi} P^0_\nu(\cos\vartheta)\sin\vartheta \mathrm{d}\vartheta d\varphi = \frac{\cos\vartheta_c P_\nu(\cos\vartheta_c) - P_{\nu+1}(\cos\vartheta_c)}{\nu}, \qquad \text{if } \nu \neq 0.$$

Hence, we replace u in equations (17) and (25) with $u_m(\vartheta, \varphi) + c(\vartheta_c, \nu, m)$, where the constant $c(\vartheta_c, \nu, m)$ is given by

$$c(\vartheta_c, \nu, m) := \begin{cases} 0 & \text{if } m \neq 0 \\ -\frac{\cos\vartheta_c P_\nu(\cos\vartheta_c) - P_{\nu+1}(\cos\vartheta_c)}{(1-\cos\vartheta_c)\nu} & \text{if } m = 0, \end{cases} \tag{27}$$

and then we solve equation (18) in terms of ε, which in turn becomes a function $\varepsilon^m_\nu(\vartheta_c)$ of the contact angle ϑ_c, parameterized by ν and m. A straightforward substitution yields

$$\varepsilon = \varepsilon^m_\nu(\vartheta_c) := \begin{cases} -(\sin\vartheta_c)^4 \frac{\left(\cot\vartheta_c\, P^m_\nu(\cos\vartheta_c) - \frac{\partial P^m_\nu(\cos\vartheta)}{\partial\vartheta}\Big|_{\vartheta_c}\right)}{(1-m^2)\, P^m_\nu(\cos\vartheta_c)}, & \text{if } m \neq 0, 1 \\ \\ -(\sin\vartheta_c)^4 \frac{\left(\cot\vartheta_c (P_\nu(\cos\vartheta_c) + c(\vartheta_c, \nu, 0)) - \frac{\partial P_\nu(\cos\vartheta)}{\partial\vartheta}\Big|_{\vartheta_c}\right)}{c(\vartheta_c, \nu, 0) + P_\nu(\cos\vartheta_c)}, & \text{if } m = 0. \end{cases} \tag{28}$$

By plotting the graphs of the functions $\varepsilon^m_\nu(\vartheta_c)$, we can decide whether the equilibrium configurations found in Section 2 are locally stable or not, with respect to specific modes. In fact, the points of the admissible region $\mathcal{A}$ that also belong to the graph of a function $\varepsilon^m_\nu(\vartheta_c)$ with $\Re e\,\nu < 1$—and $\mu < 0$—correspond to unstable equilibria of the droplet.

Before analysing the behaviour of $\varepsilon^m_\nu(\vartheta_c)$ for both signs of the line tension, we frist explore in detail the modes with $m = 1$, for which (28) looks singular. By use of the identity (*see* Equation 8.733.1 of [14])

$$(1 - x^2)\frac{\mathrm{d}P^1_\nu(x)}{\mathrm{d}x} = (\nu + 1)P^1_{\nu-1}(x) - \nu x P^1_\nu\,, \tag{29}$$

if we set $x := \cos\vartheta$ and observe that $\frac{\mathrm{d}P^1_\nu(\cos\vartheta)}{\mathrm{d}\vartheta} = -\sin\vartheta\frac{\mathrm{d}P^1_\nu(x)}{\mathrm{d}x}$, we can recast the boundary equation (18) as

$$\frac{1}{\sin\vartheta_c}[(1+\nu)P^1_{\nu-1}(\cos\vartheta_c) + (1-\nu)\cos\vartheta_c P^1_\nu(\cos\vartheta_c)] = 0$$

which is never satisfied when $\nu \neq 1$, and is identically satisfied when $\nu = 1$, that is, by (22), when $\mu = 0$. Thus, the modes $m = 1$ are marginally stable. This does not come as a surprise, since $P^1_1(\cos\vartheta)\mathrm{trig}\varphi = \sin\vartheta\mathrm{trig}\varphi$ are the projections along the droplet's normal of uniform translations along the flat substrate. Hence, the marginal modes $m = 1$ mirror the invariance under translations of the free energy functional, already noted by Sekimoto, Oguma, and Kawasaky [16].

Our statements are so far independent of the sign of line tension. Since we expect different outcomes for different signs, we split the stability analysis into two parts, by first discussing the case where the line tension is negative. Indeed, new results compared to the analysis of Widom [5] arise in this case.

III.1. Negative line tension

We start by analyzing the behaviour of $\varepsilon^m_\nu(\vartheta_c)$, when $m \geq 2$. In this way, since we already know that modes with $m = 1$ correspond to rigid translations, we are disregarding only modes with $m = 0$. We will learn in the next section that these modes only intervene when the line tension and, hence, ε is positive. We first use (29) to recast equation $(28)_1$ as

$$\varepsilon^m_\nu(\vartheta_c) = \frac{\left[(m+\nu)P^m_{-1+\nu}(\cos\vartheta_c) - (\nu-1)\cos\vartheta_c P^m_\nu(\cos\vartheta_c)\right]\sin^3\vartheta_c}{(m^2-1)P^m_\nu(\cos\vartheta_c)}\,. \tag{30}$$

For a fixed value of m, we select two arbitrary values of ν, say ν_1 and $\nu_2 > \nu_1$, with ν_1 and ν_2 different from 0 and 1, and we draw the graphs of the functions $\varepsilon^m_{\nu_1}(\vartheta_c)$ and $\varepsilon^m_{\nu_2}(\vartheta_c)$: the cases $\nu = 0$ and $\nu = 1$ need a separate treatment, since the associated Legendre function $P^m_\nu(\cos\vartheta_c)$ is identically zero when ν is an integer less than m, and so equation (30) makes no sense. Since the function $\varepsilon^m_\nu(\vartheta_c)$ depends continuously on ν, each point of the $(\vartheta_c, \varepsilon)$-plane between the graphs of $\varepsilon^m_{\nu_1}(\vartheta_c)$ and $\varepsilon^m_{\nu_2}(\vartheta_c)$ also belongs to the graph of a function $\varepsilon^m_\nu(\vartheta_c)$, for some $\nu \in (\nu_1\,,\,\nu_2)$.

By repeating this argument when m is varied, and letting ν vary in the set $\mathcal{U}$ defined in equation (23), we are able to find the pairs $(\vartheta_c, \varepsilon)$ that correspond to unstable equilibria. Figure 5 shows, for several values of m, the regions of the set

$$\mathcal{Q}_- := \{(\vartheta_c, \varepsilon) | \vartheta_c \in [0, \pi], \varepsilon < 0\}$$

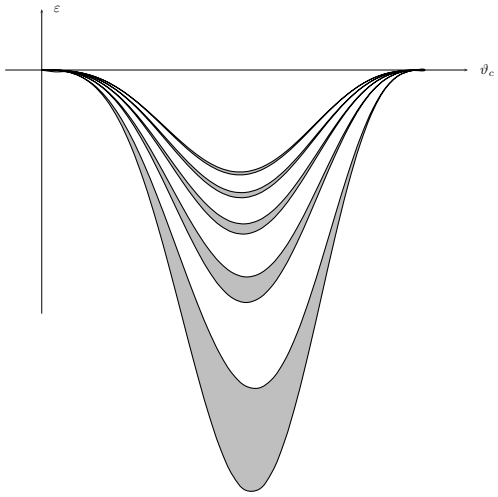

FIG. 5: Stability analysis for negative line tension. Each shaded tongue contains the graphs of the functions ε^m_ν for a fixed value of m, when ν ranges in $[-1/2, 1]$. In the limit where $m \to \infty$, the tongues tend to the ϑ_c-axis. Equilibrium pairs $(\vartheta_c, \varepsilon)$ that lie within a certain tongue—say, that corresponding to $m = m_0$– are unstable against modes associated with the spherical functions labelled by m_0. The white regions are stable against spherical functions, but they soon become unstable against modes induced by conical functions, as explained in the text.

that contain the graphs of $\varepsilon^m_\nu(\vartheta_c)$ for $\nu \in \{[-1/2\,,\,0) \cup (0\,,\,1)\} \subset \mathcal{U}$. Whenever a pair $(\vartheta_c, \varepsilon)$ falls in one of these regions, the droplet is unstable. The graph of $\varepsilon^m_\nu(\vartheta_c)$ approaches limiting curves when ν tends either to 0 or 1, though the corresponding limiting functions $\varepsilon^m_0(\vartheta_c)$ and $\varepsilon^m_1(\vartheta_c)$ fail to be in $L^2(\mathcal{S})$. By appropriately truncating the functions ε^m_ν, it is possible to construct minimizing sequences in $L^2(\mathcal{S})$ on which $\delta^2\mathcal{F}$ converges to -2 and 0, which, by (24), are the values of μ corresponding to $\nu = 0$ and $\nu = 1$, respectively. In the former case, we can conclude that the curves $\varepsilon^m_0(\vartheta_c)$ are unstable, since $\delta^2\mathcal{F}$ attains negative values arbitrarily close to -2 on the minimizing sequence. In the latter case, we conclude that the curves $\varepsilon^m_1(\vartheta_c)$ are marginal, since $\delta^2\mathcal{F}$ remains positive on the minimizing sequence, though arbitrarily close to 0.

We now have to locate in the $(\vartheta_c, \varepsilon)$-plane the curves $\varepsilon^m_{-\frac{1}{2}+\mathrm{i}\lambda}(\vartheta_c)$ which, by (23), can induce instability as well. More precisely we now prove that, for any fixed value of $m \geq 2$, the points of the $(\vartheta_c, \varepsilon)$-plane that lie below the graph of the function $\varepsilon^m_{-\frac{1}{2}}(\vartheta_c)$ also belong to the graph of a function $\varepsilon^m_{-\frac{1}{2}+\mathrm{i}\lambda}(\vartheta_c)$ for some $\lambda > 0$. In fact, it is possible to check that, when $\lambda > 0$, the graphs of $\varepsilon^m_{-\frac{1}{2}+\mathrm{i}\lambda}(\vartheta_c)$ always lie below that of $\varepsilon^m_{-\frac{1}{2}}(\vartheta_c)$ and so, since $\varepsilon^m_{-\frac{1}{2}+\mathrm{i}\lambda}(\vartheta_c)$ depends continuously on λ, we only need to prove that

$$\lim_{\lambda \to +\infty} \varepsilon^m_{-\frac{1}{2}+\mathrm{i}\lambda}(\vartheta_c) = -\infty\,. \tag{31}$$

When $m = 0$, the conical function $P_{-\frac{1}{2}+\mathrm{i}\lambda}$ has the asymptotic behaviour (*see* p. 202 of [13])

$$P_{-\frac{1}{2}+\mathrm{i}\lambda}(\cos\vartheta_c) \approx \frac{\mathrm{e}^{\lambda\vartheta_c}}{\sqrt{2\pi\lambda\sin\vartheta_c}} \tag{32}$$

when $\lambda \to +\infty$ and $0 < \eta \leq \vartheta_c \leq \pi - \eta$, with η a positive number. If, for a moment, we go back to equation $(28)_1$ we see that the asymptotic behaviour of $\varepsilon^m_{-\frac{1}{2}+\mathrm{i}\lambda}(\vartheta_c)$ when $\lambda \gg 1$ is determined by the ratio

$$\frac{1}{P^m_{-\frac{1}{2}+\mathrm{i}\lambda}} \left.\frac{\partial P^m_{-\frac{1}{2}+\mathrm{i}\lambda}(\cos\vartheta)}{\partial\vartheta}\right|_{\vartheta_c}.$$

Now, by definition,

$$P^m_\nu(\cos\vartheta_c) := (-1)^m[1-(\cos\vartheta_c)^2]^{\frac{m}{2}} \frac{\partial^m P_\nu(\cos\vartheta_c)}{\partial(\cos\vartheta_c)^m}\,. \tag{33}$$

Since asymptotic relations remain valid after differentiation, by (33) we see that the leading term in the expansion of $P^m_{-\frac{1}{2}+\mathrm{i}\lambda}(\cos\vartheta_c)$ is

$$P^m_{-\frac{1}{2}+\mathrm{i}\lambda}(\cos\vartheta_c) \approx \frac{\lambda^{(m-1/2)}\mathrm{e}^{\lambda\vartheta_c}}{\sqrt{2\pi\sin\vartheta_c}}\,,$$

while

$$\left.\frac{\partial P^m_{-\frac{1}{2}+\mathrm{i}\lambda}(\cos\vartheta)}{\partial\vartheta}\right|_{\vartheta_c} \approx \frac{\lambda^{(m+1/2)}\mathrm{e}^{\lambda\vartheta_c}}{\sqrt{2\pi\sin\vartheta_c}},$$

whence (31) follows. The reader might wonder why we insist in detecting the unstable pairs $(\vartheta_c, \varepsilon)$ throughout the set $\mathcal{Q}_-$, instead of focussing attention just on the admissible set $\mathcal{A}$. The reason is that near the origin, the set $\mathcal{A}$ is covered by graphs of the form $\varepsilon^m_{-\frac{1}{2}+\mathrm{i}\lambda}(\vartheta_c)$, with $\lambda \gg 1$. Instead of looking for an upper bound on the values of λ such that $\varepsilon^m_{-\frac{1}{2}+\mathrm{i}\lambda}(\vartheta_c)$ crosses $\mathcal{A}$, we found it convenient at this level to ignore the restrictions imposed by $\mathcal{A}$ that will be recovered at the end of the analysis.

Thus, for any prescribed value of m we can divide the set $\mathcal{Q}_-$ into two subsets $\mathcal{S}^m$ and $\mathcal{U}^m$ defined as

$$\mathcal{S}^m := \{(\vartheta_c, \varepsilon) | \vartheta_c \in (0, \pi)\ ,\ \varepsilon^m_1(\vartheta_c) < \varepsilon < 0\}$$

and

$$\mathcal{U}^m := \{(\vartheta_c, \varepsilon) | \vartheta_c \in (0, \pi)\ ,\ \varepsilon < \varepsilon^m_1(\vartheta_c)\}.$$

The continuous dependence of $\varepsilon^m_1(\vartheta_c)$ and the limit (31) suffice to prove that the equilibrium values of $(\vartheta_c, \varepsilon)$ that lie in $\mathcal{U}^m$ are unstable against modes indexed by m. To conclude that pairs $(\vartheta_c, \varepsilon)$

in $\mathcal{S}^m$ are stable we need to prove that any point in $\mathcal{S}^m$ is on the graph of a function $\varepsilon_\nu^m(\vartheta_c)$, for $\nu \in \mathcal{I} \setminus \mathcal{U}$. To this aim, it is expedient to study the roots of

$$f(\nu, \vartheta_c) := \nu(1 - \cos\vartheta_c) P_\nu(\cos\vartheta_c) + P_{\nu+1}(\cos\vartheta_c) - \cos\vartheta_c P_\nu(\cos\vartheta_c)\,, \tag{34}$$

which, by $(28)_2$, make $\varepsilon_\nu(\vartheta_c)$ diverge. Let $\bar{\vartheta}_c$ be the smallest root of (34), different from 0. When ν tends to a natural number n, the functions $P_\nu(\cos\vartheta_c)$ tend to the Legendre polynomial $P_n(\cos\vartheta_c)$ in the set $(-1+\eta, 1]$, but they have a logarithmic divergence at $\cos\vartheta_c = -1$: in fact, as a function of a complex variable, the functions $P_\nu(\cdot)$ are analytic only in the complex plane cut along $[-\infty, -1]$. As a consequence, although $f(1, \pi) \neq 0$, the first nontrivial root of $f(\nu, \vartheta_c)$ becomes closer and closer to π, when ν tends to 1, that is,

$$\lim_{\nu \to 1^+} \bar{\vartheta}_c = \pi\,.$$

On increasing ν, $\bar{\vartheta}_c$ migrates towards the left and new roots of (34) appear at $\vartheta_c = \pi$ whenever ν approaches a natural number. When $\nu \gg 1$, resort to the asymptotic expression (*cf.* formula 8.721.3 of [14])

$$P_\nu(\cos\vartheta_c) = \frac{2}{\sqrt{\pi}} \frac{\Gamma(\nu+1)}{\Gamma(\nu+\frac{3}{2})} \frac{\cos\left[\left(\nu+\frac{1}{2}\right)\vartheta_c - \frac{\pi}{4}\right]}{\sqrt{2\sin\vartheta_c}} \left[1 + O\left(\frac{1}{\nu}\right)\right]\,,$$

to Stirling's formula (see *e.g.* equation (1.4.25) of [13])

$$\Gamma(x) \approx \sqrt{2\pi} x^{x-\frac{1}{2}} e^{-x}\,,$$

and repeated use of the fundamental limit

$$\lim_{n \to +\infty} \left(1 + \frac{1}{n}\right)^n = e\,,$$

allow us to conclude that

$$f(\nu, \vartheta_c) \approx \sqrt{\frac{2\nu}{\pi}} (1 - \cos\vartheta_c) \cos\left[\left(\nu + \frac{1}{2}\right)\vartheta_c - \frac{\pi}{4}\right]\,, \qquad \text{when } \nu \gg 1$$

whence it follows that

$$\lim_{\nu \to +\infty} \bar{\vartheta}_c = 0\,.$$

Since

$$\lim_{\vartheta_c \to \bar{\vartheta}_c^{\pm}} \varepsilon_\nu(\vartheta_c) = \pm\infty\,,$$

we conclude that any point of the $(\vartheta_c, \varepsilon)$-plane – and in particular any point of the admissible set $\mathcal{A}$– apart from $(\pi, 0)$ belongs to the graph of some function $\varepsilon_\nu(\vartheta_c)$, at least for sufficiently

large values of ν. This in turn proves that the minimum eigenvalue $\mu_{\min}$ of equations (17)-(18) has a positive value at all points in the set $\mathcal{S}^m$ which thus correspond to locally stable equilibria. Moreover, since $\mu_{\min} = 0$ along the curves $\varepsilon_1^m(\vartheta_c)$ is 0, it is now legitimate to call them the *marginal curves*, as they separate regions that are stable against the modes indexed by m from regions that are unstable against the same modes.

As remarked in the Introduction, when the line tension is negative, functional (1) is unbounded from below. We thus expect that no equilibrium configuration can be stable when m is large enough, and so the perturbing modes make the contact line wigglier and wigglier. To substantiate this claim, we study the behaviour of the marginal curves $\varepsilon_1^m(\vartheta_c)$ as m increases. We first note that, by use of de l'Hôpital's rule in equation (30),

$$\varepsilon_1^m(\vartheta_c) := \lim_{\nu\to 1} \varepsilon_\nu^m(\vartheta_c) = (\sin\vartheta_c)^3 \frac{\left.\frac{\partial P_\nu^m}{\partial\nu}\right|_{\nu=0}}{(m-1)\left.\frac{\partial P_\nu^m}{\partial\nu}\right|_{\nu=1}}, \tag{35}$$

where we observed that $\left.\frac{\partial P_{\nu-1}^m}{\partial\nu}\right|_{\nu=1} = \left.\frac{\partial P_\nu^m}{\partial\nu}\right|_{\nu=0}$. Strictly speaking, equation (35) holds only away from $\vartheta_c = \pi$, where P_ν^m diverges. This point, however, does not concern us here, since we only consider partial wetting. Since (see eqs. 8.762.1 and 8.762.3 of [14])

$$\left.\frac{\partial P_\nu(\cos\vartheta_c)}{\partial\nu}\right|_{\nu=0} = 2\log\cos\frac{\vartheta_c}{2}$$

and

$$\left.\frac{\partial P_\nu^{-1}(\cos\vartheta_c)}{\partial\nu}\right|_{\nu=1} = -\frac{1}{2}\tan\frac{\vartheta_c}{2}\left(\sin\frac{\vartheta_c}{2}\right)^2 + \sin\vartheta_c\log\cos\frac{\vartheta_c}{2}\,,$$

by use of the identity (*cf.* eq. 8.752.2 of [14])

$$P_\nu^{-1}(\cos\vartheta_c) = -\frac{\Gamma(\nu)}{\Gamma(\nu+2)}P_\nu^1 = \frac{P_\nu^1}{\nu(\nu+1)}$$

we readily obtain that

$$\left.\frac{\partial P_\nu^1(\cos\vartheta_c)}{\partial\nu}\right|_{\nu=1} = \tan\frac{\vartheta_c}{2}\left(\sin\frac{\vartheta_c}{2}\right)^2 - 2\sin\vartheta_c\log\cos\frac{\vartheta_c}{2}\,.$$

Thus, by recalling definition (33) and interchanging the order of differentiation, we see from (35) that $\varepsilon_1^m(\vartheta_c)$ behaves as $1/m$, when $m \gg 1$, and so

$$\lim_{m\to\infty}\varepsilon_1^m(\vartheta_c) = 0\,,$$

which proves our assertion.

To put this result in the right perspective we recall that upon increasing m, the typical length $\mathcal{L}_m(\vartheta_c)$, over which oscillations associated with the modes labelled by m manifest themselves,

decreases. When $\mathcal{L}_m(\vartheta_c)$ becomes smaller than the characteristic length $|\xi|$, the mode lacks any physical relevance because it induces deformations at length scales that lie beyond the range of validity of the model. For a fixed value of m we adopt the following, global definition of the length $\mathcal{L}_m(\vartheta_c)$

$$\mathcal{L}_m(\vartheta_c) := \left(\frac{\int_{\mathcal{S}} |u_m|^2 \mathrm{d}A}{\int_{\mathcal{S}} |\nabla_{\mathrm{s}} u_m|^2 \mathrm{d}A} \right)^{1/2} , \tag{36}$$

where $u_m(\vartheta, \varphi)$ is the limit of $P_\nu^m(\cos\vartheta)\sin(m\varphi)$ when $\nu \to 1$, that is, the marginal curve associated with the mode m. Wild oscillations of the surface-gradient $\nabla_{\mathrm{s}} u_m$ of the perturbation u_m lower $\mathcal{L}_m(\vartheta_c)$, which thus appears as a reasonable candidate to measure the corrugation of the contact line induced by the mode u_m. The analysis built in this section enables us to determine, for any fixed equilibrium point $(\bar\vartheta_c, \bar\varepsilon)$, the smallest value $\bar m$ of m for which the equilibrium is unstable against $u_{\bar m}$. Thus, if $\mathcal{L}_{\bar m}(\bar\vartheta_c) < |\xi|$ the mode is physically irrelevant, and we refer to $(\bar\vartheta_c, \bar\varepsilon)$ as a *conditionally stable* equilibrium, since the instability becomes apparent on a length inaccessible to the model.

By using standard formulae in vector analysis, we can give (36) the following form

$$\mathcal{L}_m(\vartheta_c) = R \left[\frac{\int_0^{2\pi} \int_0^{\vartheta_c} |u_m|^2 \, \sin\vartheta \mathrm{d}\vartheta \mathrm{d}\varphi}{\int_0^{2\pi} \int_0^{\vartheta_c} |\frac{\partial u_m}{\partial \vartheta} + \frac{1}{\sin\vartheta} \frac{\partial u_m}{\partial \varphi}|^2 \sin\vartheta \mathrm{d}\vartheta \mathrm{d}\varphi} \right]^{1/2} , \tag{37}$$

whence, by setting

$$\mathcal{I}_m(\vartheta_c) := -\frac{\mathcal{L}_m(\vartheta_c)}{R} , \tag{38}$$

and recalling that ξ is negative when the line tension is negative, we can rephrase the condition $\mathcal{L}_{\bar m}(\bar\vartheta_c) < |\xi|$ as

$$\varepsilon < \mathcal{I}_{\bar m}(\bar\vartheta_c) . \tag{39}$$

Let us consider the set $\bar{\mathcal{M}} \subset \mathcal{Q}_-$ bounded by the graphs of $\varepsilon_1^{\bar m - 1}(\vartheta_c)$ and $\varepsilon_1^{\bar m}(\vartheta_c)$. The graph of $\varepsilon = \mathcal{I}_{\bar m}(\vartheta_c)$ splits the set $\bar{\mathcal{M}}$ in two or three subsets (*see* Fig. 6): while the regions above $\varepsilon = \mathcal{I}_{\bar m}(\vartheta_c)$ are unaffected by the criterion (39), the region below $\varepsilon = \mathcal{I}_{\bar m}(\vartheta_c)$, though potentially unstable, becomes conditionally stable by virtue of (39). It is crucial to note (6) that instability remains effective when the contact angle is small. As we learnt in Section 2, equilibria with small values of the contact angle exist when the line tension has high strength. We thus conclude that conditionally stable equilibria exist provided that the line tension strength is not too high, in agreement with the results found in [9] for a different morphology.

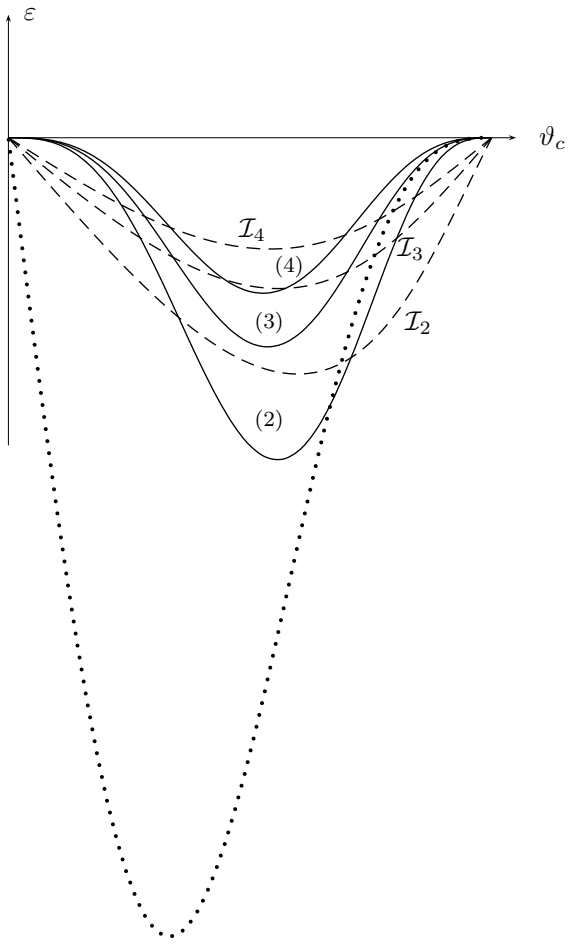

FIG. 6: Conditionally stable equilibria. The solid lines are three marginal curves: (2) is $\varepsilon_1^2(\vartheta_c)$, (3) is $\varepsilon_1^3(\vartheta_c)$, and (4) is $\varepsilon_1^4(\vartheta_c)$. The dashed curves are the graphs of $\varepsilon = \mathcal{I}_2(\vartheta_c)$, $\varepsilon = \mathcal{I}_3(\vartheta_c)$, and $\varepsilon = \mathcal{I}_4(\vartheta_c)$. For a given value of m, the region below the marginal curve $\varepsilon_1^m(\vartheta_c)$ would be unstable with respect to modes labelled by m. However, modes below the curve $\varepsilon = \mathcal{I}_m(\vartheta_c)$ are effective at a length scale outside the realm of validity of the model, and so their instability is fictitious: the equilibrium is conditionally stable against modes labelled by m. As remarked in the text, as the line tension strength increases, the equilibrium contact angle becomes smaller and smaller. Hence, the representative point falls in a region in which (39) is violated, and so instability persists.

III.2. Positive line tension

We just proved that modes with $m \geq 2$ are effective when the line tension, and so ε, is negative. Moreover, modes with $m = 1$ and $\nu = 1$ are associated with rigid translations of the droplet. Hence, when the line tension is positive, we can restrict attention to modes with $m = 0$, for which the function $\varepsilon_\nu^0(\vartheta_c)$ is defined through equation $(28)_2$, with $c(\vartheta_c, \nu, 0)$ given by $(27)_2$. By proceeding as in Subsection 3.1, we conclude that the set of the $(\vartheta_c, \varepsilon)$-plane bounded by the graphs of $\varepsilon_1(\vartheta_c)$

and $\varepsilon_{-\frac{1}{2}}(\vartheta_c)$ corresponds to unstable equilibria, with $\varepsilon_1(\vartheta_c)$ playing the rôle of marginal curve. With only technical changes, we can still prove that the set of the $(\vartheta_c, \varepsilon)$-plane above the graph of $\varepsilon_{-\frac{1}{2}}(\vartheta_c)$ contains the graph of $\varepsilon_{-\frac{1}{2}+\mathrm{i}\lambda}(\vartheta_c)$, for some positive value of λ. To this aim, we show that

$$\lim_{\lambda\to+\infty} \varepsilon_{-\frac{1}{2}+\mathrm{i}\lambda}(\vartheta_c) = +\infty$$

and use the continuous dependence of $\varepsilon_\nu(\vartheta_c)$ on ν. A glance at equation $(28)_2$ suffices to conclude that the leading term of $\varepsilon_{-\frac{1}{2}+\mathrm{i}\lambda}(\vartheta_c)$ is

$$\varepsilon_{-1/2+\mathrm{i}\lambda}(\vartheta_c) \approx (\sin\vartheta_c)^3 \frac{\left.\frac{\partial P_{-\frac{1}{2}+\mathrm{i}\lambda}}{\partial\vartheta}\right|_{\vartheta=\vartheta_c}}{c(\vartheta_c,\nu,0) + P_{-\frac{1}{2}+\mathrm{i}\lambda}} .$$

If we use the following identity (*see* eq. 8.733.1 of [14])

$$(\nu+1)P_{\nu+1}(x) = (\nu+1)xP_\nu(x) - (1-x^2)\frac{\mathrm{d}P_\nu(x)}{\mathrm{d}x} , \tag{40}$$

to eliminate $P_{\nu+1}$ from $c(\vartheta_c,\nu,0)$ in equation $(27)_2$, and then resort to the asymptotic expansion (32), we can prove that $\varepsilon_{-\frac{1}{2}+\mathrm{i}\lambda}(\vartheta_c)$ diverges with λ, when $\lambda\to+\infty$.

Finally, the arguments used in Subsection 3.1 make us confident that the points below the graph of $\varepsilon_1(\vartheta_c)$ correspond to locally stable equilibria, since there the minimum value of μ is positive. Hence, the curve $\varepsilon_1(\vartheta_c)$ is indeed a marginal curve, when the line tension is positive. As already shown in Section 2, for a given value ϑ_c^0 of the bare contact angle, there is a critical value $\delta_c(\vartheta_c^0)$ of δ such that, if $\delta > \delta_c(\vartheta_c^0)$ there are two equilibria and there is none, if $\delta < \delta_c(\vartheta_c^0)$. Figure 7 shows the graph of the marginal curve superimposed to the admissible set $\mathcal{A}$: only the subset of $\mathcal{A}$ below the curve $\varepsilon_1(\vartheta_c)$ contains stable equilibria: thus, whenever, for given values of ϑ_c^0 and δ, two equilibria exist, only the one with the lower value of ϑ_c is stable. We also note that the two equilibria coalesce along the marginal curve $\varepsilon_1(\vartheta_c)$.

The modes that mark the transition from stable to unstable equilibria have normal component u proportional to $P_1(\cos\vartheta) + c = \cos\vartheta + c$. Hence, we conclude that equation (10) maps spheres into spheres, as it should be in this case, since the stability threshold we found here agrees with Widom's [5] though we have not selected spherical perturbations from the very beginning of our analysis.

III.3. Reverse mapping

In the previous sections we learnt how to find locally stable equilibria in the $(\vartheta_c, \varepsilon)$-plane, where it was easier to solve equations (17)-(18). However, both ϑ_c and ε are not constitutive parameters.

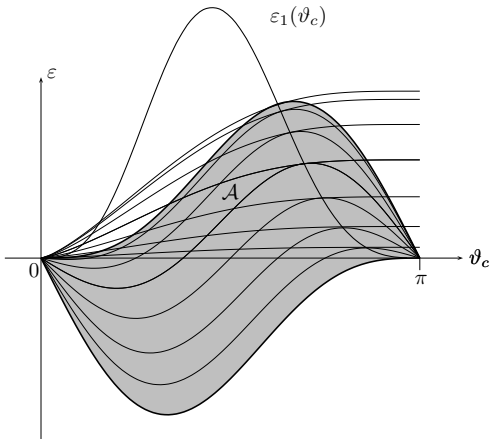

FIG. 7: The marginal curve $\varepsilon_1(\vartheta_c)$ divides the admissible set $\mathcal{A}$ into two parts. Only the part below the graph of $\varepsilon_1(\vartheta_c)$ is stable. The thin lines are graphs of the functions $\varepsilon_1(\vartheta_c, \vartheta_c^0)$ and $\varepsilon_2(\vartheta_c, \delta_c(\vartheta_c^0))$ defined in (8), for several values of ϑ_c^0. When $\delta = \delta_c(\vartheta_c^0))$, the two equilibria coalesce into one another and so $\varepsilon_1(\vartheta_c, \vartheta_c^0)$ and $\varepsilon_2(\vartheta_c, \delta_c(\vartheta_c^0))$ have a common tangent. Here we see that the marginal curve $\varepsilon_1(\vartheta_c)$ passes through these tangent points.

Thus, it is appropriate to translate our results into the $(\cos\vartheta_c^0, \delta)$-plane since, by (4) and (7), these parameters are easily related to the constitutive parameters τ, γ, and w, as well as to the volume V of the droplet. To achieve this aim, we need to find a function

$$f : (\vartheta_c, \varepsilon) \mapsto (\cos\vartheta_c^0, \delta)$$

that maps solutions of equations (8) into the $(\cos\vartheta_c^0, \delta)$-plane. We will refer to f as to the *reverse mapping*. To find the reverse mapping we solve equation (8) with respect to $\cos\vartheta_c^0$ and δ, obtaining

$$\cos\theta_c^0 = \frac{\varepsilon}{\sin\theta_c} + \cos\theta_c \tag{41}$$

$$\delta = \frac{2 + (\cos\theta_c)^3 - 3\cos\theta_c}{\varepsilon^3}. \tag{42}$$

Then, the image of the function $\varepsilon_\nu^m(\vartheta_c)$ is the parametric curve

$$f(\varepsilon_\nu^m(\vartheta_c)) = \left(\cos\vartheta_c^0\left(\vartheta_c, \varepsilon_\nu^m(\vartheta_c)\right), \delta\left(\vartheta_c, \varepsilon_\nu^m(\vartheta_c)\right)\right).$$

The reverse mapping works in completely different ways, according to the sign of the line tension. In fact, (41) can work as an inverse map only when the line tension is negative since only in that case, for a given value of the pair $(\cos\vartheta_c^0, \delta)$, a unique pair $(\vartheta_c, \varepsilon)$ solves (8). Figure 8 shows several marginal curves in the $(\cos\vartheta_c^0, \delta)$-plane, obtained by mapping the curves $\varepsilon_1^m(\vartheta_c)$ found in Subsection 3.1, together with the corresponding unstable sets.

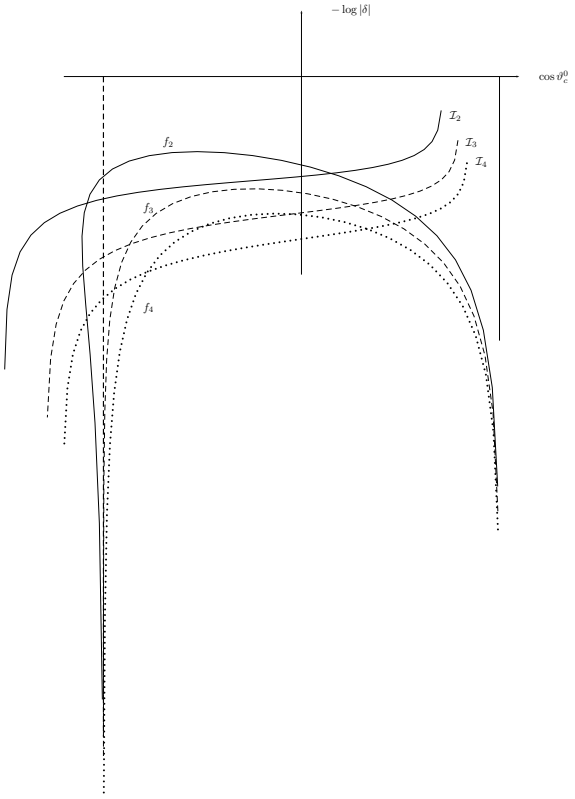

FIG. 8: The reverse mapping of three marginal curves $f_m := f(\varepsilon_\nu^m(\vartheta_c))$, corresponding to $m = 2$, 3 and 4, are plotted together with the reverse mappings $\mathcal{I}_i$ of the curves $\mathcal{I}_m$ that determine the admissible modes. While, if no restriction is imposed on the modes, the whole region above the marginal curve corresponding to a particular value of m would be unstable, the criterion (39) restricts the set of unstable modes to those lying below the curve $\mathcal{I}_m$. We stress that on the vertical axis we plotted $\lambda := -\log_{10}|\delta|$, so that the limit of extremely high and negative line tension corresponds to $\lambda \to +\infty$. All the curves $\mathcal{I}_m$ diverge at $\lambda = +\infty$ when $\cos\vartheta_c^0 \to 1$. For completeness, we drawn the curves f_m and $\mathcal{I}_m$ also beyond the value $\cos\vartheta_c^0 = -1$.

On the other hand, when the line tension is positive, there is no way to use (41) as the inverse of (8) since, for a given value of $(\cos\vartheta_c^0, \delta)$, the solutions are either two or none. To extract information from the reverse mapping, we recall that along the marginal curve $\varepsilon_1(\vartheta_c)$ the two equilibria coalesce in one. We map $\varepsilon_1(\vartheta_c)$ back into the $(\cos\vartheta_c^0, \varepsilon)$-plane, obtaining the curve shown in Figure 9. This curve, whose dashed part is unphysical as it lies outside the admissible set, separates the region $\mathcal{N}$, where no equilibria exist, from the region $\mathcal{T}$, where two equilibria exist, for any admissible pair $(\cos\vartheta_c^0, \delta)$. However, at variance with the previous case, we cannot extract further information on the stability of the equilibria since any point in $\mathcal{T}$ corresponds to two solutions. Furthermore, since an equilibrium configuration in $\mathcal{T}$ is unstable, when ν ranges in $\mathcal{U}$ the reverse mappings of $\varepsilon_\nu(\vartheta_c)$ cover the set $\mathcal{T}$ and curves corresponding to different values of ν never intersect each other. The

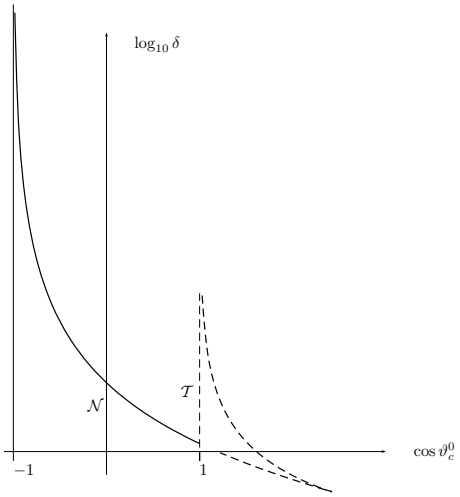

FIG. 9: The reverse mapping of the marginal curve $\varepsilon_1(\vartheta_c)$. To have a better graphic layout, we plotted $\log_{10}\delta$ on the vertical axis. The solid portion is the part of the marginal curve lying in the admissible set $\mathcal{A}$: it has an asymptote at $\cos\vartheta_c^0 = -1$ and leaves the admissible set at $\cos\vartheta_c^0 = 1$ and $\log_{10}\delta = 0.1723$. The dashed line is the part of the marginal curve that lies outside $\mathcal{A}$; consequently, unphysical values of $\cos\vartheta_c^0 > 1$ are obtained. In the set $\mathcal{T}$ two equilibria coexist, while no equilibria exist in $\mathcal{N}$.

same remark holds for the reverse mappings of the curves $\varepsilon_\nu(\vartheta_c)$, when $\nu > 1$.

IV. CONCLUSIONS

In this paper we performed the stability analysis of the equilibria of a sessile droplet lying upon a rigid, flat, and homogeneous substrate, in the presence of line tension. As expected, we obtain different outcomes according to the sign of the line tension. While our analysis strengthens the results obtained by Widom in [5] when the line tension is positive, qualitatively new results occur when the line tension is negative. While we confirm that no equilibrium can definitely be stable, we introduce a natural cutoff on the admissible modes, by selecting only the modes that are effective at a length-scale compatible with the realm of validity of our model. In this way we are able to show that, when the strength of the line tension is not too high, negative values of the line tension are compatible with the existence of (conditionally) stable equilibria. This paper opens the way to a natural generalization in which the effects of line tension are coupled with the curvature of the substrate. This study is indeed currently pursued and will be published elsewhere [15].

Acknowledgments

It is a pleasure to acknowledge the Istituto di Matematica Applicata e Tecnologie Informatiche (I.M.A.T.I.) del C.N.R-Pavia for its support to this work.

---

[1] A. Amirfazli, A.W. Neumann, Status of the three-phase line tension, *Adv. Colloid Interf. Sci.* **110** (2004), 121-141.

[2] J.W. Gibbs, On the equilibrium of heterogeneous substances. In *The Collected Papers of J. Willard Gibbs* Vol. I, 55-353. London: Yale University Press, (1957).

[3] D.J. Steigmann & D. Li, Energy-minimizing states of capillary systems with bulk, surface, and line phases. *IMA J. Appl. Math.* **55** (1995), 1-17.

[4] G. Alberti, G. Bouchitté, and P. Seppecher, Phase transition with the line-tension effect. *Arch. Ration. Mech. An.* **144**, (1998), 1-46.

[5] B. Widom, Line tension and the shape of a sessile drop. *J. Chem. Phys.* **99** (1995), 2803-2806.

[6] V.G. Baidakov, G. Sh. Boltachev, & G.G. Chernykh, Curvature corrections to surface tension. *Phys. Rev. E* **70** (2004), 011603.

[7] L. Boruvka, & A.W. Neumann, Generalization of the classical theory of capillarity. *J. Chem. Phys.* **66** (1977), 5464-5476.

[8] R. Rosso & E.G. Virga, Local stability for a general wetting functional. *J. Phys. A: Math. Gen.* **37** (2004), 3989-4015. Corrigendum, *ibid.* **37** (2004), 8751.

[9] R. Rosso & E.G. Virga, Sign of line tension in liquid bridge stability. *Phys. Rev. E* **70** (2004), 031603.

[10] P. Lenz & R. Lipowsky, Stability of droplets and channels on homogeneous and structured surfaces. *Eur. Phys. J. E* **1** (2000), 249-262.

[11] M.P. do Carmo, *Differential Geometry of Curves and Surfaces.* Prentice-Hall: Englewood-Cliffs (1976).

[12] F. Baginski, Upper and lower bounds for eigenvalues of the Laplacian on a spherical cap, *Quart. J. Appl. Math.* **48** (1990), 569-573. Errata, *ibid.* **49** (1991), 399.

[13] N.N. Lebedev, *Special Functions and their Applications.* Dover: New York (1972).

[14] I.S. Gradshteyn, and I.M. Ryzhik, *Table of Integrals, Series, and Products.* Fifth Edn., A. Jeffrey Ed. Academic Press: San Diego (1994).

[15] L. Guzzardi & R. Rosso, Stability of wetting on curved substrates: effects of line tension. *In preparation*, (2004).

[16] K. Sekimoto, R. Oguma, and K. Kawasaki, Morphological stability analysis of partial wetting. *Adv. Phys.* **176** (1987), 359-392.